Asian Journal of Chemistry; Vol. 36, No. 12 (2024), 2870-2878

ASIAN JOURNAL OF CHEMISTRY

https://doi.org/10.14233/ajchem.2024.32688

Novel Pyrimidine Tethered Benzamide Derivatives as Potential Anticancer Agents: Synthesis, Characterization, Molecular Docking and *In vitro* Cytotoxicity Evaluation

K. JYOTHI* and M. KANNADASAN

Faculty of Pharmaceutical Sciences, Motherhood University, Dehradun Road, Village Karoundi Post-Bhagwanpur, Roorkee-247661, India

*Corresponding author: E-mail: jyothikasapogu214@gmail.com

Received: 13 September 2024; *Accepted*: 4 November 2024; *Published online*: 30 November 2024; AJC-21829

Current research work presents the synthesis, characterization, molecular docking study and *in vitro* cytotoxicity evaluation of novel pyrimidine-tethered benzamide derivatives as potential anticancer agents. The synthesis involved multi-steps procedure, including the synthesis of various chalcones (**3a-t**) with corresponding ketones (**1** and **2**) and substituted aldehydes (**a-j**), followed by pyrimidine amines (**5a-t**) with condensation of chalcones and guanidine and finally pyrimidinyl benzamide derivatives (**8a-t**) from compounds **5a-t** coupling with acid chloride (**7**) using DIBAL-H. Synthesized compounds characterized by NMR spectroscopy and HRMS. The molecular docking studies were conducted against EGFR (6LUD) and CDK-4 (7SJ3) receptors, revealing distinct binding affinities influenced by substituent groups. Additionally, the cytotoxicity of the synthesized compounds was evaluated using the MTT assay against various cancer cell lines, including A-549 (non-small cell lung cancer), HCT-116 (colorectal cancer), PANC-1 (pancreatic cancer) and HaLa (cervical cancer), along with one normal human embryonic kidney cell line (HEK-293). Among the synthesized compounds, derivatives **8f** and **8j** exhibited the best anticancer activity against A-549 cells, compounds **8j** and **8e** showed exceptional potency against HCT-116 cells, compounds **8f** and **8j** demonstrated high efficacy against PANC-1 cells and compound **8h** displayed remarkable potency against HaLa cells. The findings highlight the potential of these pyrimidinyl benzamide derivatives as targeted anticancer agents.

Keywords: Pyrimidinyl-benzamides, Anticancer activity, Cell lines, MTT Assays, EGFR, CDK-4.

INTRODUCTION

The estimated total number of new cases of cancer in 2023 was 20.01 million, with 9.6 million people losing their lives to the disease [1]. Despite a lot of progress and high-tech improvements in cancer treatments around the world, cancer is still a widespread illness that poses a health risk to people [2,3]. Chemotherapy is acknowledged as a significant practical approach due to its comparative effectiveness with other treatments, *etc*. [4,5]. Although several anticancer chemotherapeutic drugs have proven to be effective in treating different 32 significant concern for both patients and physicians. Present endeavors to mitigate the adverse effects induced by anticancer drugs have proven effective in most cases, encompassing surgical interventions and radiation impacts. However, these approaches fall short in adequately addressing potential long-term repercussions [6]. To tackle and surmount this challenge, it is imperative to develop innovative anticancer medications that specifically target cancer cells, offering enhanced safety profiles and efficacy.

Research institutions and the pharmaceutical industry are diligently creating novel anticancer medications that target specific cells, effectively combat cancer and possess the capability to trigger selective responses. Furthermore, the development of decisive chemotherapeutic agents is impeded by two fundamental challenges: the striking resemblances between normal and malignant cells and the diverse characteristics of tumors. These obstacles underline the complexity of producing effective treatments tailored to target cancer cells while sparing healthy ones [7]. Consequently, the medical and pharmaceutical industries are continuously dedicated to researching and developing new anticancer drugs.

Among the crucial nitrogen containing heterocyclic frameworks, the pyrimidine nucleus is emerging as a significant candidate for cancer targeting. Pazopanib, nilotinib, imatinib

and dasatinib are four notable anticancer drugs, recognized for their efficacy, that incorporate the pyrimidine nucleus as a central structural motif (Fig. 1) [8]. These medications primarily function by targeting the superfamily of tyrosine kinase-linked pathways, particularly inhibiting the activity of epidermal growth factor receptor tyrosine kinase (EGFR-TK) in cancer cells. They achieve this by blocking the autophosphorylation of the epidermal growth factor receptor and the transmission of signals stimulated by epidermal growth factor (EGF) [9,10]. The epidermal growth factor receptor, commonly referred to as EGFR, stands out as a prominent target of tyrosine kinase inhibitors, receiving extensive research attention [11,12]. Tyrosine kinases serve as vital enzymes pivotal in cell proliferation, differentiation, metastasis and survival. The uncontrolled activation of these enzymes and the overproduction of EGFR, stemming from mutations throughout the expression process, contribute to the development of various cancers including breast, prostate, ovarian, lung and brain tumors [13].

The pyrimidine scaffold also holds significant importance in the context of cyclin-dependent kinase 4 (CDK-4) inhibition, primarily in the development of anticancer agents. CDK-4 is a crucial enzyme involved in cell cycle regulation, particularly in the G1 phase, where it plays a key role in controlling cell division. Inhibition of CDK-4 can lead to cell cycle arrest, making it an attractive target for cancer therapy [14]. Given the pivotal role of the EGFR-TK and CDK-4 pathways in the genesis of various cancers, numerous research institutions are directing their efforts toward crafting novel anticancer drugs tailored to inhibit these pathways specifically.

Recognizing the pivotal role of pyrimidine derivatives in directly inhibiting the EGFR-TK and CDK-4 pathways, endeavors were initiated to develop novel organic compounds centered around the pyrimidine ring structure. These compounds were subsequently evaluated for their cytotoxicity *in vitro* against four different cancer cell lines alongside a normal human cell line. Furthermore, the molecular docking techniques were employed to explore the molecular interactions between the designed derivatives and the targets EGFR and CDK-4, aiming to uncover potential underlying mechanisms.

EXPERIMENTAL

All synthetic-grade chemicals and solvents used in this study were purchased from Sigma-Aldrich, Bangalore, India, without additional purification. Merck-precoated aluminium TLC plates coated with silica gel 60 F_{254} were used for reaction monitoring and achieved visualization with iodine vapours in a UV chamber. Melting points were determined using Remi electronic melting point equipment. ^{1}H and ^{13}C NMR spectra were recorded on a Bruker DRX instrument with chemical shift values (δ) relative to the internal standard, tetramethyl silane, reported in ppm. The HRMS spectra were captured using a Waters Xevo Q-Tof Mass spectrometer.

Synthesis of pyrimidinyl benzamides: The scheme of synthesis for the designed pyrimidinyl benzamide derivative is displayed in **Scheme-I**.

Synthesis of chalcone: Substituted ketone (**1** or **2**) (0.01 mol) and corresponding aldehydes (**a-j**) (0.01 mol) were combined in a reaction mixture, stirred for 2-3 h in 5-10 mL of methanol, followed by the gradual addition of 10 mL of 40% NaOH solution with continuous stirring at room temperature. The reaction mixture was left overnight at room temperature, then poured into ice-cold water and acidified with hydrochloric acid. The resulting precipitated substituted chalcone (**3**) was filtered, dried and subsequently recrystallized from methanol [15].

Synthesis of pyrimidine amine: A solution containing substituted chalcone (**3a-t**) (0.01 mol) in 50 mL of methanol was combined with 0.01 mol of potassium hydroxide and 40 mL of a 0.25 M solution of guanidine hydrochloride (**4**), then refluxed for 3-4 h. Following reflux, the reaction mixture was cooled and acidified with a few drops of HCl (20 mL of 0.5 M solution). The resulting precipitate, pyrimidine amine (**5a-t**), was isolated, dried and subsequently recrystallized from methanol [16].

Conversion of aryl acid to acid chloride: Benzoic acid (**6**) (1 mmol; 1 equiv.) was dissolved in 0.70 mL of $SOCl_2$ (10 mmol; 10 equiv.) in a 10 mL vial equipped with a magnetic stir bar at room temperature. Then, water (18 µL; 1 mmol; 1 equiv.) was added and the vial was capped with a Teflon-lined cap,

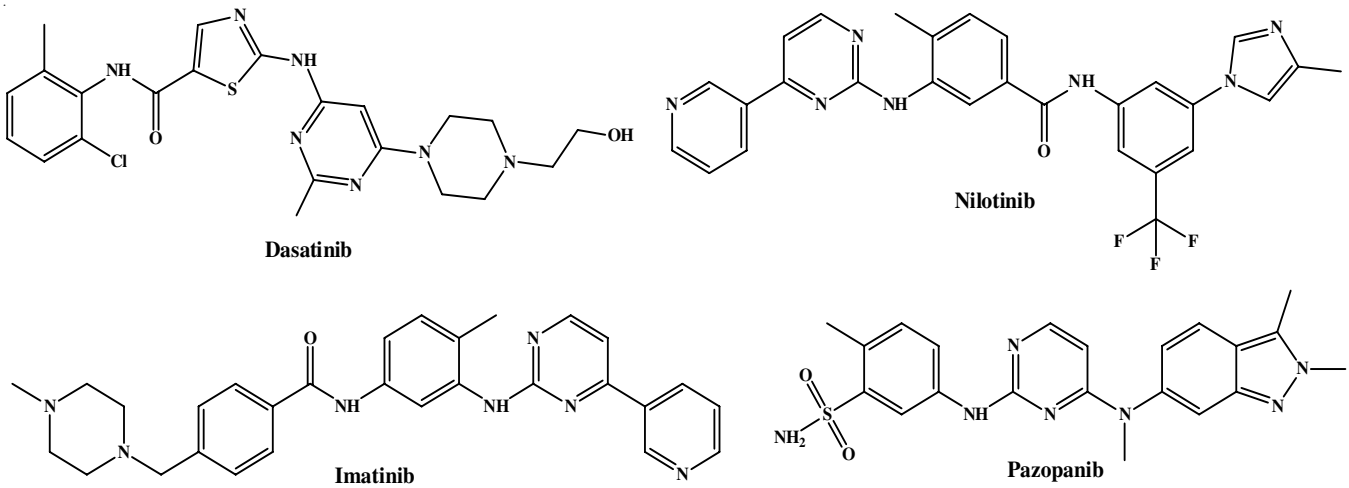

Fig. 1. Marketed anticancer drugs with pyrimidine scaffold

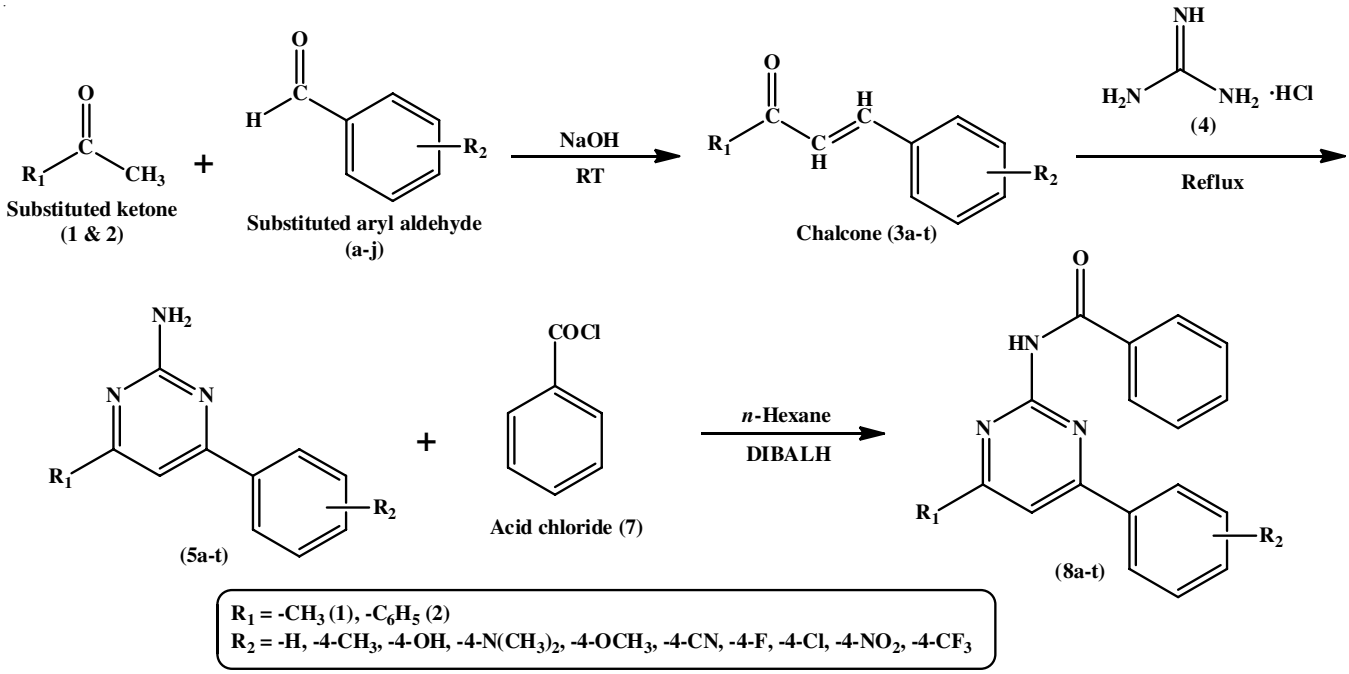

Scheme-I: Synthesis of substituted pyrimidinyl benzamides (**8a-t**)

ensuring it was never filled more than 40% to prevent the risk of rupture. The reaction mixture was stirred until gas evolution was observed. Following this, the cap was cautiously removed and toluene (1 mL) was added to the vial. The mixture was subsequently subjected to reduced pressure to facilitate the azeotropic removal of $SOCl_2$, resulting in the formation of the desired product, benzoyl chloride (**7**) [17].

General procedure for synthesis of pyrimidine amide: A dry and argon-flushed flask, equipped with a magnetic stirring bar and a septum, was charged with pyrimidine amine (**5a-t**) (1.25 mmol) and THF (10 mL). After cooling to 0 ºC, DIBALH (1.0 M in hexane, 1.2 mmol) was added dropwise and the mixture was stirred for 3 h at the same temperature. Substituted aryl chloride (1.0 mmol) was added slowly to the reaction mixture, which was stirred for 10 min. The reaction was stopped with aqueous 1 N HCl (10 mL) and extracted with diethyl ether (2 × 10 mL). The combined organic layers were dried over $MgSO_4$, filtered and concentrated under reduced pressure. Purification of the residue by column chromatography on silica gel yielded final product of substituted pyrimidinyl benzamides (**8a-t**) [18].

***N*-(4-Methyl-6-phenylpyrimidin-2-yl)benzamide (8a):** Pale yellow solid, yield: 78.2%; m.p.: 161-162 ºC; ^{1}H NMR (500 MHz, DMSO-d_6) δ ppm: 10.46 (s, 1H), 8.19-8.13 (m, 2H), 7.96 (dt, *J* = 7.9, 1.2 Hz, 2H), 7.58-7.46 (m, 6H), 7.46-7.39 (m, 1H), 7.29 (s, 1H), 2.44 (d, *J* = 0.7 Hz, 3H); ^{13}C NMR (125 MHz, DMSO-d_6) δ ppm: 169.60, 164.86, 160.15, 156.79, 137.40, 133.95, 132.00, 129.68, 129.07, 128.52, 128.11, 127.66, 110.60, 23.94. HRMS for $C_{11}H_{12}N_4O_2$: : *m/z* ([M + H]$^+$): 290.1209, found 290.1206.

***N*-(4-Methyl-6-(*p*-tolyl)pyrimidin-2-yl)benzamide (8b):** Pale yellow solid, yield: 74.1%; m.p.: 169-170 ºC; ^{1}H NMR (500 MHz, DMSO-d_6) δ ppm: 10.46 (s, 1H), 7.96 (dt, *J* = 7.9, 1.2 Hz, 2H), 7.58-7.45 (m, 5H), 7.28 (s, 1H), 7.19-7.14 (m, 2H), 2.44 (d, *J* = 0.7 Hz, 3H), 2.34 (d, *J* = 0.9 Hz, 3H); ^{13}C NMR (125 MHz, DMSO-d_6) δ ppm: 132.00, 128.95, 128.52, 128.11, 127.20, 110.62, 23.94, 21.23. HRMS for $C_{19}H_{17}N_3O$: *m/z* ([M + H]$^+$) 304.1417, found 304.1417.

***N*-(4-(4-Hydroxyphenyl)-6-methylpyrimidin-2-yl)-benzamide (8c):** Pale yellow solid, yield: 79.4%; m.p.: 165-166 ºC; ^{1}H NMR (500 MHz, DMSO-d_6) δ ppm: 10.50 (s, 1H), 9.60 (s, 1H), 7.96 (dt, *J* = 7.9, 1.2 Hz, 2H), 7.84-7.77 (m, 2H), 7.58-7.53 (m, 1H), 7.53-7.45 (m, 2H), 7.30 (s, 1H), 6.94-6.88 (m, 2H), 2.40 (d, *J* = 0.7 Hz, 3H); ^{13}C NMR (125 MHz, DMSO-d_6) δ ppm: 132.00, 128.98 (d, *J* = 5.9 Hz), 128.52, 128.11, 116.06, 110.79, 23.94. HRMS for $C_{18}H_{15}N_3O_2$: *m/z* ([M + H]$^+$) 306.1245, found 306.1243.

***N*-(4-(4-(Dimethylamino)phenyl)-6-methylpyrimidin-2-yl)benzamide (8d):** Pale yellow solid, yield: 82.6%; m.p.: 217-218 ºC; ^{1}H NMR (500 MHz, DMSO-d_6) δ ppm: 10.53 (s, 1H), 7.96 (dt, *J* = 7.8, 1.1 Hz, 2H), 7.89-7.83 (m, 2H), 7.58-7.45 (m, 3H), 7.31 (s, 1H), 6.81-6.75 (m, 2H), 3.04 (s, 6H), 2.51 (s, 3H); ^{13}C NMR (125 MHz, DMSO-d_6) δ ppm: 132.00, 128.52, 128.13 (d, *J* = 4.8 Hz), 112.18, 110.66, 40.30, 23.94. HRMS for $C_{20}H_{20}N_4O$: *m/z* ([M + H]$^+$) 333.1678, found 333.1672.

***N*-(4-(4-Methoxyphenyl)-6-methylpyrimidin-2-yl)-benzamide (8e):** Pale yellow solid, yield: 75.7%; m.p.: 182-183 ºC; ^{1}H NMR (500 MHz, DMSO-d_6) δ ppm: 10.49 (s, 1H), 7.99-7.93 (m, 2H), 7.77-7.71 (m, 2H), 7.58-7.52 (m, 1H), 7.52-7.45 (m, 2H), 7.30 (s, 1H), 6.95-6.89 (m, 2H), 3.79 (s, 3H), 2.44 (d, *J* = 0.7 Hz, 3H); ^{13}C NMR (125 MHz, DMSO-d_6) δ ppm: 132.00, 128.83, 128.52, 128.11, 114.01, 110.79, 55.34, 23.94. HRMS for $C_{19}H_{17}N_3O$: *m/z* ([M + H]$^+$) 320.1374, found 320.1368.

N-(4-(4-Cyanophenyl)-6-methylpyrimidin-2-yl)-benzamide (8f): Pale yellow solid, yield: 71.5%; m.p.: 229-230 ºC; ^{1}H NMR (500 MHz, DMSO-d_6) δ ppm: 10.42 (s, 1H), 7.99-7.90 (m, 4H), 7.75-7.69 (m, 3H), 7.58-7.53 (m, 1H), 7.53-7.45 (m, 2H), 2.39 (d, *J* = 0.7 Hz, 3H); ^{13}C NMR (125 MHz,

DMSO-d_6) δ ppm: 132.59, 132.00, 128.52, 128.07 (d, J = 8.5 Hz), 110.66, 23.94. HRMS for $C_{19}H_{14}N_4O$: *m/z* ([M + H]$^+$) 315.1243, found 315.1241.

***N*-(4-(4-Fluorophenyl)-6-methylpyrimidin-2-yl)-benzamide (8g):** Pale yellow solid, yield: 81.3%; m.p.: 178-179 ºC; ^{1}H NMR (500 MHz, DMSO-d_6) δ ppm: 10.44 (s, 1H), 7.99-7.93 (m, 2H), 7.85-7.78 (m, 2H), 7.58-7.53 (m, 1H), 7.53-7.45 (m, 2H), 7.32 (s, 1H), 7.31-7.22 (m, 2H), 2.48 (s, 3H); ^{13}C NMR (125 MHz, DMSO-d_6) δ ppm: 132.00, 131.79 (d, J = 3.5 Hz), 129.53 (d, J = 9.0 Hz), 128.52, 128.11, 115.53, 115.35, 110.79, 23.94. HRMS for $C_{18}H_{14}FN_3O$: *m/z* ([M + H]$^+$) 308.1119, found 308.1114.

***N*-(4-(4-Chlorophenyl)-6-methylpyrimidin-2-yl)-benzamide (8h):** Off white solid, yield: 77.8%; m.p.: 185-186 ºC; ^{1}H NMR (500 MHz, DMSO-d_6) δ ppm: 10.47 (s, 1H), 7.99-7.91 (m, 4H), 7.58-7.45 (m, 3H), 7.36-7.30 (m, 3H), 2.42 (d, J = 0.7 Hz, 3H); ^{13}C NMR (125 MHz, DMSO-d_6) δ ppm: 132.00, 129.24, 128.60 (d, J = 19.1 Hz), 128.11, 110.66, 23.94. HRMS for $C_{18}H_{14}ClN_3O$: *m/z* ([M + H]$^+$): 324.0997, found 324.0988.

***N*-(4-Methyl-6-(4-nitrophenyl)pyrimidin-2-yl)benzamide (8i):** Pale brown solid, yield: 75.4%; m.p.: 204-205 ºC; ^{1}H NMR (500 MHz, DMSO-d_6) δ ppm: 10.41 (s, 1H), 8.23-8.17 (m, 2H), 8.13-8.07 (m, 2H), 7.99-7.93 (m, 2H), 7.72 (s, 1H), 7.58-7.53 (m, 1H), 7.53-7.45 (m, 2H), 2.40 (d, J = 0.7 Hz, 3H); ^{13}C NMR (125 MHz, DMSO-d_6) δ ppm: 132.00, 128.52, 128.12 (d, J = 3.1 Hz), 124.17, 110.67, 23.94. HRMS for $C_{18}H_{14}N_4O_3$: *m/z* ([M + H]$^+$): 335.1093, found 335.1092.

***N*-(4-Methyl-6-(4-(trifluoromethyl)phenyl)pyrimidin-2-yl)benzamide (8j):** Pale yellow solid, yield: 72.1%; m.p.: 196-197 ºC; ^{1}H NMR (500 MHz, DMSO-d_6) δ ppm: 10.53 (s, 1H), 7.99-7.93 (m, 2H), 7.82-7.76 (m, 2H), 7.72 (d, J = 1.0 Hz, 1H), 7.66 (dq, J = 11.5, 1.4 Hz, 2H), 7.58-7.45 (m, 3H), 2.50 (s, 3H); ^{13}C NMR (125 MHz, DMSO-d_6) δ ppm: 132.00, 128.52, 128.19-127.79 (m), 125.40 (q, J = 4.6 Hz), 110.63, 23.94. HRMS for $C_{19}H_{14}F_3N_3O$: *m/z* ([M + H]$^+$) 358.1127, found 358.1124.

***N*-(4,6-Diphenylpyrimidin-2-yl)benzamide (8k):** Pale yellow solid, yield: 73.9%; m.p.: 191-192 ºC; ^{1}H NMR (500 MHz, DMSO-d_6) δ ppm: 10.68 (s, 1H), 8.18 (s, 1H), 7.95 (ddd, J = 7.5, 6.1, 1.4 Hz, 6H), 7.58-7.46 (m, 8h), 7.46-7.39 (m, 2H); ^{13}C NMR (125 MHz, DMSO-d_6) δ ppm: 169.60, 159.88, 157.15, 137.65, 133.90, 132.00, 129.68, 129.07, 128.52, 128.11, 127.94, 107.84. HRMS for $C_{23}H_{17}N_3O$: *m/z* ([M + H]$^+$): 352.1419, found 352.1417.

***N*-(4-Phenyl-6-(*p*-tolyl)pyrimidin-2-yl)benzamide (8l):** Pale yellow solid, yield: 70.7%; m.p.: 215-216 ºC; ^{1}H NMR (500 MHz, DMSO-d_6) δ ppm: 10.65 (s, 1H), 8.04-7.95 (m, 5H), 7.94 (d, J = 1.4 Hz, 1H), 7.58-7.45 (m, 6H), 7.19-7.14 (m, 2H), 2.34 (d, J = 0.7 Hz, 3H); ^{13}C NMR (125 MHz, DMSO-d_6) δ ppm: 132.00, 129.68, 129.01 (d, J = 14.9 Hz), 128.52, 128.11, 127.94, 127.46, 107.82, 21.23. HRMS for $C_{24}H_{19}N_3O$: *m/z* ([M + H]$^+$): 366.1631, found 366.1631.

***N*-(4-(4-Hydroxyphenyl)-6-phenylpyrimidin-2-yl)-benzamide (8m):** Pale yellow solid, yield: 71.3%; m.p.: 207-208 ºC; ^{1}H NMR (500 MHz, DMSO-d_6) δ ppm: 10.68 (s, 1H), 9.54 (s, 1H), 8.17 (s, 1H), 7.99-7.91 (m, 4H), 7.90-7.84 (m, 2H), 7.58-7.46 (m, 6H), 7.46-7.39 (m, 1H), 6.94-6.88 (m, 2H); ^{13}C NMR (125 MHz, DMSO-d_6) δ ppm: 169.60, 159.80 (d, J = 18.8 Hz), 159.09, 157.16, 137.65, 133.90, 132.00, 129.68, 129.33-128.98 (m), 128.52, 128.11, 127.94, 116.07, 107.89. HRMS for $C_{23}H_{17}N_3O_2$: *m/z* ([M + H]$^+$) 368.1381, found 368.1377.

***N*-(4-(4-(Dimethylamino)phenyl)-6-phenylpyrimidin-2-yl)benzamide (8n):** Pale yellow solid, yield: 76.5%; m.p.: 243-244 ºC; ^{1}H NMR (500 MHz, DMSO-d_6) δ ppm: 10.72 (s, 1H), 8.17 (s, 1H), 7.99-7.91 (m, 5H), 7.91-7.85 (m, 2H), 7.58-7.48 (m, 6H), 7.48-7.39 (m, 1H), 6.80-6.75 (m, 2H), 2.97 (s, 6H); ^{13}C NMR (125 MHz, DMSO-d_6) δ ppm: 169.60, 159.88, 159.22, 157.16, 151.77, 137.65, 133.90, 132.00, 129.86, 129.68, 129.07, 128.48 (d, J = 10.7 Hz), 128.11, 127.94, 112.17, 107.80, 40.30. HRMS for $C_{25}H_{22}N_4O_2$: *m/z* ([M + H]$^+$) 395.1807, found 395.1804.

***N*-(4-(4-Methoxyphenyl)-6-phenylpyrimidin-2-yl)-benzamide (8o):** White solid, yield: 70.1%; m.p.: 217-218 ºC; ^{1}H NMR (500 MHz, DMSO-d_6) δ ppm: 10.68 (s, 1H), 8.16 (s, 1H), 7.99-7.91 (m, 4H), 7.80-7.74 (m, 2H), 7.58-7.46 (m, 6H), 7.46-7.39 (m, 1H), 6.95-6.89 (m, 2H), 3.79 (s, 3H); ^{13}C NMR (125 MHz, DMSO-d_6) δ ppm: 132.00, 129.67 (d, J = 3.7 Hz), 129.05 (d, J = 4.1 Hz), 128.52, 128.11, 127.94, 114.01, 107.89, 55.34. HRMS for $C_{24}H_{19}N_3O_2$: *m/z* ([M + H]$^+$): 382.1521, found 382.1519.

***N*-(4-(4-Cyanophenyl)-6-phenylpyrimidin-2-yl)-benzamide (8p):** Pale yellow solid, yield: 69.2%; m.p.: 266-267 ºC; ^{1}H NMR (500 MHz, DMSO-d_6) δ ppm: 10.68 (s, 1H), 8.20 (s, 1H), 7.99-7.91 (m, 6H), 7.75-7.69 (m, 2H), 7.58-7.46 (m, 6H), 7.46-7.39 (m, 1H); ^{13}C NMR (125 MHz, DMSO-d_6) δ ppm: 169.60, 159.88, 159.20, 157.16, 137.65, 136.27, 133.90, 132.59, 132.00, 129.68, 129.07, 128.52, 128.28, 128.11, 127.94, 118.03, 111.83, 107.81. HRMS for $C_{24}H_{16}N_4O$: *m/z* ([M + H]$^+$): 377.1399, found 377.1395.

***N*-(4-(4-Fluorophenyl)-6-phenylpyrimidin-2-yl)-benzamide (8q):** Pale yellow solid, yield: 76.2%; m.p.: 239-240 ºC; ^{1}H NMR (500 MHz, DMSO-d_6) δ ppm: 10.65 (s, 1H), 8.21 (s, 1H), 7.99-7.91 (m, 4H), 7.86-7.80 (m, 2H), 7.58-7.46 (m, 6H), 7.46-7.39 (m, 1H), 7.30-7.22 (m, 2H); ^{13}C NMR (125 MHz, DMSO-d_6) δ ppm: 169.60, 159.88, 159.36, 157.16, 137.65, 133.90, 132.10-131.84 (m), 129.88-129.59 (m), 129.07, 128.52, 128.11, 127.94, 115.53, 115.35, 107.88. HRMS for $C_{23}H_{16}FN_3O$: *m/z* ([M + H]$^+$) 370.1286, found 370.1284.

***N*-(4-(4-Chlorophenyl)-6-phenylpyrimidin-2-yl)-benzamide (8r):** White solid, yield: 72.8%; m.p.: 209-210 ºC; ^{1}H NMR (500 MHz, DMSO-d_6) δ ppm: 10.68 (s, 1H), 8.18 (s, 1H), 8.05-7.99 (m, 2H), 7.99-7.91 (m, 4H), 7.58-7.46 (m, 6H), 7.46-7.39 (m, 1H), 7.36-7.30 (m, 2H); ^{13}C NMR (125 MHz, DMSO-d_6) δ ppm: 169.60, 159.88, 159.64, 157.16, 137.65, 135.09, 133.85 (d, J = 13.8 Hz), 132.00, 129.68, 129.48, 129.07, 128.60 (d, J = 19.1 Hz), 128.11, 127.94, 107.81. HRMS for $C_{23}H_{16}ClN_3O$: *m/z* ([M + H]$^+$): 386.1061, found 386.1059.

***N*-(4-(4-Nitrophenyl)-6-phenylpyrimidin-2-yl)benzamide (8s):** Pale brown solid, yield: 75.7%; m.p.: 216-217 ºC; ^{1}H NMR (500 MHz, DMSO-d_6) δ ppm: 10.68 (s, 1H), 8.20 (dd, J = 8.3, 1.4 Hz, 3H), 8.17-8.11 (m, 2H), 7.99-7.91 (m, 4H), 7.58-7.46 (m, 6H), 7.46-7.39 (m, 1H): ^{13}C NMR (125 MHz, DMSO-d_6) δ ppm: 169.60, 159.82 (d, J = 13.8 Hz), 157.15,

146.67, 138.15, 137.65, 133.90, 132.00, 129.68, 129.07, 128.57 (d, J = 10.9 Hz), 128.11, 127.94, 124.19, 107.92. HRMS for $C_{22}H_{16}N_4O_3$: *m/z* ([M + H]$^+$): 397.1330, found 397.1323.

***N*-(4-Phenyl-6-(4-(trifluoromethyl)phenyl)pyrimidin-2-yl)benzamide (8t):** Pale yellow solid, yield: 70.3%; m.p.: 228-229 ºC; ^{1}H NMR (500 MHz, DMSO-d_6) δ ppm: 10.68 (s, 1H), 8.21 (s, 1H), 7.99-7.91 (m, 4H), 7.84-7.77 (m, 2H), 7.66 (dq, J = 11.5, 1.4 Hz, 2H), 7.58-7.46 (m, 6H), 7.46-7.39 (m, 1H); ^{13}C NMR (125 MHz, DMSO-d_6) δ ppm: 169.60, 159.88, 158.60, 157.16, 137.65, 136.21, 133.90, 132.75 (q, J = 32.0 Hz), 132.00, 129.68, 129.07, 128.52, 128.25-127.77 (m), 125.40 (q, J = 4.6 Hz), 107.82. HRMS for $C_{24}H_{16}F_3N_3O$: *m/z* ([M + H]$^+$) 420.1302, found 420.1302.

Molecular docking: The X-ray crystal structures of EGFR (6LUD) and two CDK-4 (7SJ3) domains were obtained from the Protein Data Bank. The protein preparation wizard module of Schrödinger software was used to prepare the protein complex by introducing hydrogen atoms and allocating bond orders to the 3D structure of protein. The LigPrep module of Schrödinger software was used to prepare ligands with defined chirality and optimize their 3D structures using the OPLS 2005 force field. The receptor sites for 6LUD and 7SJ3 were analyzed using the SITEMAP ANALYSIS TOOL of Maestro 11.8 and receptor grids were generated using the grid generation tool of Schrödinger suite. The Molecular docking was performed using the Glide program's extra-precision docking modes (Glide XP) and the XP Glide score was calculated using the binding interaction energy, van der Waals energy, electrostatic potential energy and strain energy. The binding interaction of the ligands to the active site of EGFR and CDK-4 was examined using Schrödinger Maestro interface [19].

MTT assay: The cytotoxicity and cell viability of 1*H*-1,2,4-triazole-3-carboxamide derivatives (**4a-n**) were assessed using the MTT (3-(4,5-dimethylthiazol-2-yl)-2,5-diphenyl-tetrazolium bromide) assay. Several human cancer cell lines, such as A-549 (non-small cell lung cancer), HCT-116 (colorectal cancer), PANC-1 (pancreatic cancer) and HaLa (cervical cancer), along with one normal human embryonic kidney cell line (HEK-293), were cultured in 96-well plates and given time to adhere overnight. Subsequently, the cells were subjected to different concentrations (0.1 µM, 10 µM, 50 µM and 100 µM) of the synthesized 1*H*-1,2,4-triazole-3-carboxamide derivatives **4a-n** for incubation periods of 24, 48 or 72 h. After the designated incubation period, the MTT solution was introduced into each well and the plates were subsequently incubated to facilitate the formation of formazan crystals. The formazan crystals were solubilized in DMSO and the absorbance was quantified using a microplate reader. The relationship between absorbance values and cell viability was analyzed, where lower absorbance values correlated with increased cytotoxicity and reduced cell viability. Data obtained from the MTT assay across different concentrations and time points were scrutinized to determine the half-maximal inhibitory concentration (IC_{50}) values of the 1*H*-1,2,4-triazole-3-carboxamide derivatives for each cell line. The experiments were replicated three times, including suitable controls to validate the precision and consistency of the assay results [20].

RESULTS AND DISCUSSION

All the compounds were synthesized successfully from the designed synthetic route (**Scheme-I**) and the yield were good. The proton NMR spectra of the compounds displayed a singlet peak around the chemical shift region of 9.5 to 9.8 ppm that confirm the carboxamide bond formation in the final step that yielded the substituted pyrimidinyl benzamide derivatives. Furthermore, the ^{13}C NMR of the compounds disclosed the carbonyl carbon peak around 160-170 ppm.

Molecular docking study: Table-1 outlines the molecular docking scores of novel pyrimidinyl benzamide derivatives (**8a-t**) with the 6LUD and 7SJ3 receptors.

TABLE-1
RESULTS OF DOCKING STUDY OF NOVEL PYRIMIDINYL BENZAMIDE DERIVATIVES (**8a-t**)

Compd.	R_1	R_2	Docking scores	
			6LUD	7SJ3
8a	-CH_3	-H	-5.428	-6.402
8b	-CH_3	-4-CH_3	-6.442	-6.352
8c	-CH_3	-4-OH	-4.939	-8.254
8d	-CH_3	-4-$N(CH_3)_2$	-5.967	-5.976
8e	-CH_3	-4-OCH_3	-5.45	-7.019
8f	-CH_3	-4-CN	-5.589	-4.883
8g	-CH_3	-4-F	-4.201	-6.657
8h	-CH_3	-4-Cl	-5.877	-5.738
8i	-CH_3	-4-NO_2	-4.099	-5.461
8j	-CH_3	-4-CF_3	-4.11	-5.718
8k	-C_6H_5	-H	-3.918	-4.863
8l	-C_6H_5	-4-CH_3	-2.665	-4.214
8m	-C_6H_5	-4-OH	-5.397	-6.925
8n	-C_6H_5	-4-$N(CH_3)_2$	-3.002	-5.363
8o	-C_6H_5	-4-OCH_3	-3.647	-3.817
8p	-C_6H_5	-4-CN	-3.183	-6.348
8q	-C_6H_5	-4-F	-3.581	-6.105
8r	-C_6H_5	-4-Cl	-3.902	-4.956
8s	-C_6H_5	-4-NO_2	-3.445	-4.717
8t	-C_6H_5	-4-CF_3	-4.055	-4.845
Osimertinib (co-crystallized ligand of 6LUD)			-5.952	–
Abemaciclib (co-crystallized ligand of 7SJ3)			–	-7.541

Docking analysis of 6LUD

Methyl-substituted derivatives (8a-j): The docking scores for the synthesized compounds against 6LUD range from -6.442 to -4.099. Compounds **8b** (-6.442, R_2: 4-CH_3) (Fig. 2) and **8d** (-5.967, R_2: 4-$N(CH_3)_2$), with 4-CH_3 and 4-$N(CH_3)_2$ substituents, respectively, displayed the highest binding affinities, suggesting strong interactions with the 6LUD protein. Compounds **8a** (-5.428, R_2: -H), **8e** (-5.45, R_2: 4-OCH_3), **8g** (-4.201, R_2: 4-F) and **8h** (-5.877, R_2: -4-Cl) exhibited moderate binding affinities. Compound **8f** (-5.589, R_2: 4-CN), with 4-CN substitution, showed a lower binding affinity.

The electronic nature of the R_2 substituents plays a crucial role in the binding affinities. In the high-affinity cases of **8b** and **8d**, the electron-donating nature of 4-CH_3 and 4-$N(CH_3)_2$ groups likely enhances favourable interactions with the 6LUD binding site. Conversely, the moderate and low-affinity cases, featuring electron-withdrawing groups like 4-F, 4-Cl, 4-NO_2

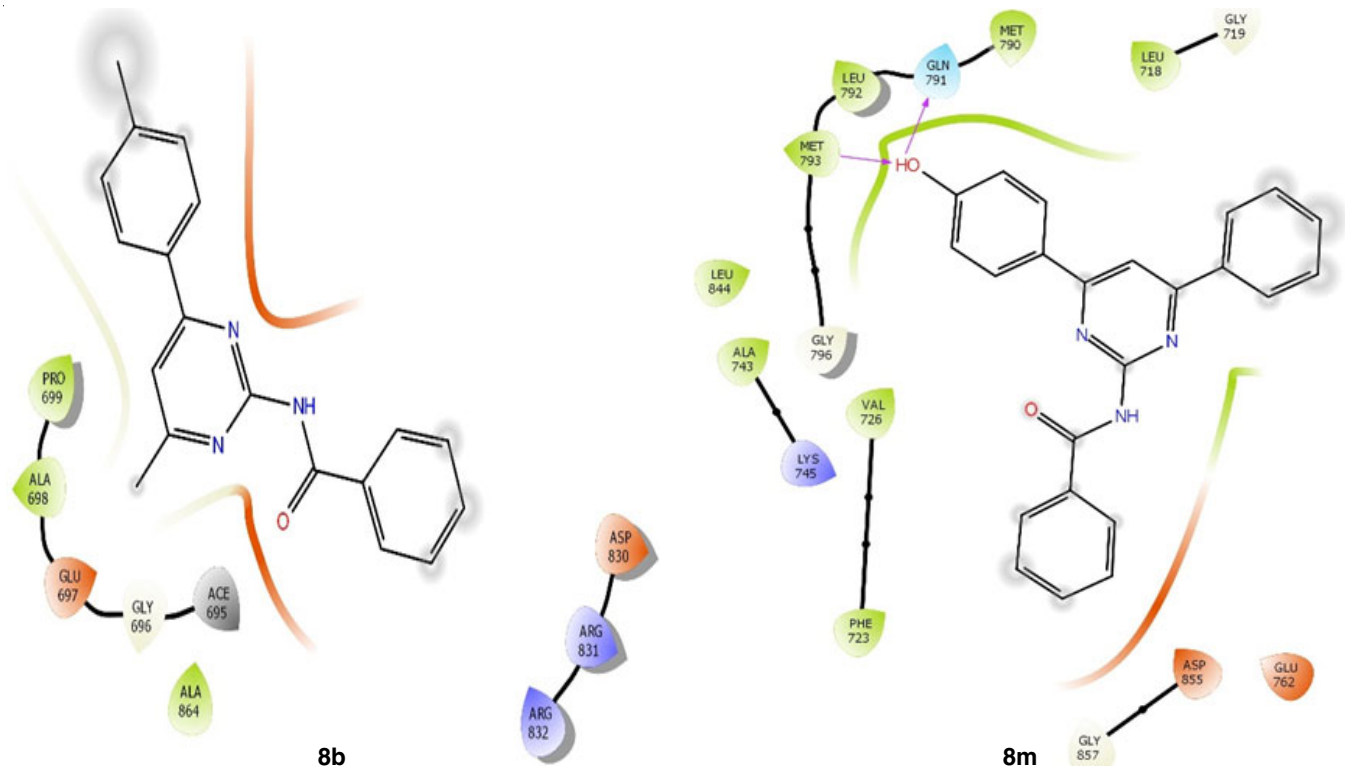

Fig. 2. Ligand interactions of **8b** and **8m** with 6LUD

and 4-CN, show reduced binding affinities, possibly due to less favourable electronic interactions.

Phenyl-ring derivatives (8k-t): Compound **8m** (-5.397), with a 4-OH substituent (Fig. 2) demonstrated the highest binding affinity, emphasizing the crucial role of electron-donating groups in facilitating strong interactions. The presence of an -OH group likely enhances hydrogen bonding and electrostatic interactions, contributing to the overall binding affinity. Compounds **8o** (-3.647), **8n** (-3.002) and **8k** (-3.918), featuring 4-OCH_3, 4-$N(CH_3)_2$ and -H substituents, respectively, displayed moderate binding affinities. The electron-donating nature of these substituents supports favourable interactions with the 6LUD binding site.

Significantly, compounds **8l** (-2.665), **8q** (-3.581) and **8r** (-3.902), incorporating -4-CH_3, -4-F and -4-Cl substituents, respectively, exhibited relatively lower binding affinities. The electron-withdrawing nature of these substituents may diminish interactions with the 6LUD binding site.

Docking analysis of 7SJ3

Methyl-substituted derivatives (8a-j): The docking scores for the compounds against 7SJ3 range from -8.254 to -4.883. Compound **8c** (-8.254, R_2: -4-OH), with -4-OH substitution (Fig. 3), displayed the highest binding affinity, indicating strong interactions with the 7SJ3 protein.

Compounds **8a** (-6.442, R_2: -H), **8f** (-6.352, R_2: 4-CN), **8g** (-4.883, R_2: 4-F), **8h** (-5.738, R_2: 4-Cl), **8i** (-5.461, R_2: 4-NO_2) and **8j** (-5.718, R_2: 4-CF_3) exhibited moderate binding affinities. Compounds **8e** (-7.019, R_2: 4-OCH_3), **8k** (-3.918, R_2: -H), **8l** (-2.665, R_2: 4-CH_3), **8m** (-5.397, R_2: 4-OH), **8n** (-3.002, R_2: 4-$N(CH_3)_2$), **8o** (-3.647, R_2: 4-OCH_3), **8p** (-3.183, R_2: 4-CN), **8q** (-3.581, R_2: 4-F), **8r** (-3.902, R_2: 4-Cl), **8s** (-3.445, R_2: 4-NO_2) and **8t** (-4.055, R_2: 4-CF_3) displayed lower binding affinities.

Similar to the 6LUD case, the electronic nature of R_2 significantly impacts binding affinities for 7SJ3. High-affinity cases, such as **8c** with -4-OH, suggest that electron-donating groups contribute positively to interactions. Conversely, moderate and low-affinity cases, featuring electron-withdrawing groups like 4-F, 4-Cl, 4-NO_2 and -4-CN, show reduced binding affinities, possibly due to less favourable electronic interactions.

Phenyl-ring derivatives (8k-t): Compound **8m** (-6.925), featuring a 4-OH substituent (Fig. 3), displayed the highest binding affinity against 7SJ3, highlighting the favourable impact of electron-donating groups on ligand-protein interactions. The presence of -OH likely enhances hydrogen bonding and contributes to a robust binding affinity. Compounds **8r** (-4.956), **8t** (-4.845) and **8s** (-4.717), incorporating 4-Cl, 4-CF_3 and 4-NO_2 substituents, respectively, demonstrated moderate binding affinities. The electron-withdrawing nature of these substituents suggests a complex interplay between electronic effects and binding interactions. Compound **8l** (-4.214), with a 4-CH_3 substituent, also displayed a strong binding affinity against 7SJ3, indicating the nuanced influence of substituent nature.

The docking study of novel pyrimidinyl benzamide derivatives (**8a-t**) against 6LUD and 7SJ3 reveals distinct patterns in binding affinities associated with variations in the R_1 and R_2 substituents. Compounds with similar R_2 substituents displayed varying affinities against 6LUD and 7SJ3, emphasizing the target-specific nature of ligand interactions. For example, compound **8m** with 4-OH exhibited high affinity for both targets, while compound **8l** with 4-CH_3 showed strong affinity primarily for 7SJ3. Compounds with electron-donating groups like -OH,

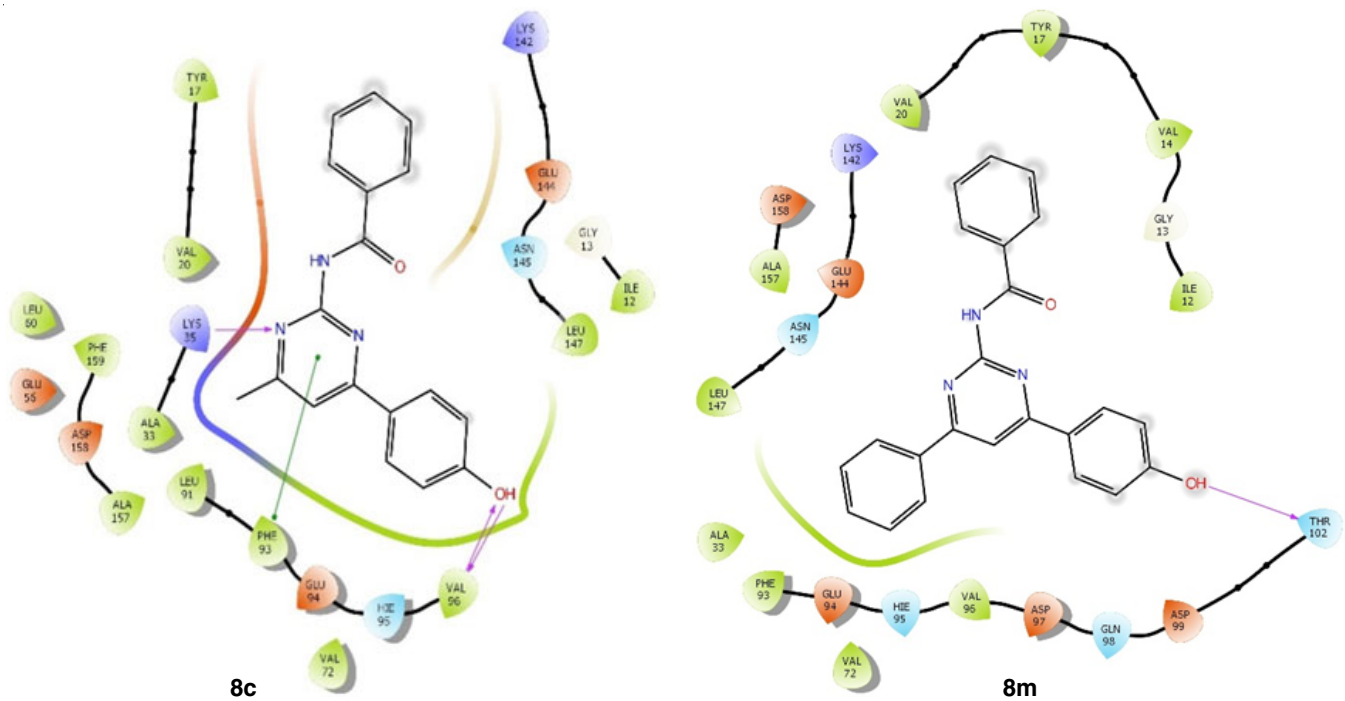

Fig. 3. Ligand interactions of **8c** and **8m** with 7SJ3

-OCH_3 and -$N(CH_3)_2$ generally showed higher affinity for 7SJ3 compared to 6LUD. Electron-withdrawing groups like -NO_2 and -CF_3 displayed weaker binding to both targets.

This docking study demonstrates the potential of pyrimidinyl benzamides (**8a-t**) as scaffolds for targeted cancer therapy. By fine-tuning the R_1 and R_2 substituents, it is possible to modulate the binding affinities and target specificity of these compounds. Based on the results, compounds **8b**, **8d**, **8m** and **8p** warrant further investigation through *in vitro* and *in vivo* studies to validate their potential as therapeutic agents.

Anticancer activity: The results of the MTT assay of pyrmidinyl benzamide derivatives (**8a-t**) in terms of IC_{50} values are enumerated in Table-2. Both 4-methyl (**8a**-**j**) and 4-phenyl (**8k**-**t**) derivative displayed good to moderate cytotoxicity against the tested cancer cell lines and comparatively disclosed low cytotoxic potential towards the normal human embryonic kidney

TABLE-2
IC_{50} VALUES OF SYNTHESIZED PYRIMIDINYL BENZAMIDE DERIVATIVES (**8a-t**) FROM MTT ASSAY

Compound	Non-small cell lung cancer line (A-549)	Colorectal cancer cell line (HCT-116)	Pancreatic cancer cell line (PANC-1)	Cervical cancer cell line (HaLa)	Human embryonic kidney cell line (HEK-293)
8a	13.37 ± 2.14	13.50 ± 1.30	11.74 ± 0.92	14.88 ± 1.85	37.21 ± 4.94
8b	15.17 ± 1.08	11.98 ± 1.07	14.02 ± 2.13	14.55 ± 1.07	35.39 ± 2.19
8c	13.64 ± 2.18	13.77 ± 1.33	11.97 ± 0.94	15.23 ± 1.89	37.96 ± 4.99
8d	15.45 ± 1.11	12.23 ± 1.09	14.29 ± 2.17	14.86 ± 1.09	36.14 ± 2.24
8e	10.06 ± 1.83	4.95 ± 1.82	6.90 ± 1.09	11.98 ± 4.18	31.21 ± 4.99
8f	6.24 ± 1.91	10.30 ± 1.22	6.75 ± 1.09	14.39 ± 2.79	30.57 ± 3.40
8g	14.34 ± 3.25	12.34 ± 1.77	10.20 ± 2.12	16.45 ± 2.70	39.71 ± 1.47
8h	11.42 ± 1.28	16.22 ± 1.32	9.70 ± 1.14	8.07 ± 2.11	39.18 ± 1.27
8i	24.00 ± 4.19	23.91 ± 2.31	20.71 ± 3.47	30.76 ± 3.74	42.92 ± 1.75
8j	9.87 ± 1.79	4.85 ± 1.79	6.75 ± 1.06	11.76 ± 4.09	30.56 ± 4.94
8k	20.24 ± 1.34	19.31 ± 1.51	21.07 ± 2.12	28.12 ± 1.24	43.28 ± 1.01
8l	22.41 ± 3.23	18.43 ± 1.22	22.03 ± 4.04	27.10 ± 1.74	34.30 ± 3.59
8m	23.00 ± 2.85	20.42 ± 3.29	24.47 ± 1.54	19.80 ± 3.63	39.94 ± 1.79
8n	16.03 ± 2.05	18.99 ± 1.21	17.47 ± 1.08	18.89 ± 2.79	36.58 ± 1.40
8o	21.70 ± 2.33	17.54 ± 3.29	25.67 ± 2.66	20.15 ± 3.74	38.47 ± 1.75
8p	19.47 ± 1.30	16.72 ± 2.17	19.17 ± 1.20	18.97 ± 1.16	36.81 ± 2.72
8q	18.23 ± 3.25	18.15 ± 1.51	17.97 ± 2.11	28.04 ± 2.69	43.27 ± 1.18
8r	19.80 ± 1.31	18.88 ± 1.48	20.63 ± 2.07	27.52 ± 1.22	42.37 ± 0.99
8s	21.25 ± 2.28	17.15 ± 3.22	25.13 ± 2.60	19.68 ± 3.64	37.64 ± 1.71
8t	19.08 ± 1.27	16.36 ± 2.12	18.76 ± 1.17	18.53 ± 1.13	36.05 ± 2.67
Doxorubicin (ref. std.)	1.28 ± 0.65	1.45 ± 0.89	1.89 ± 0.74	1.63 ± 0.91	2.95 ± 0.72

cell line (HEK-293) than the reference standard doxorubicin revealing their safety towards the normal cell lines.

Non-small cell lung cancer line (A-549): For the A-549 cell lines the IC_{50} values for 4-methyl derivatives range from 6.24 ± 1.91 (compound **8f**) to 24.00 ± 4.19 (compound **8i**). Lower IC_{50} values, such as 6.24 ± 1.91 for **8f** and 9.87 ± 1.79 for **8j**, indicate higher potency in inhibiting the proliferation of non-small cell lung cancer cells. Compound **8i**, with an IC_{50} value of 24.00 ± 4.19, has a higher concentration requirement for 50% inhibition, suggesting lower potency compared to other 4-methyl derivatives.

The IC_{50} values for 4-phenyl derivatives range from 16.03 ± 2.05 (compound **8n**) to 23.00 ± 2.85 (compound **8m**). Lower IC_{50} values, such as 16.03 ± 2.05 for **8n** and 18.23 ± 3.25 for **8q**, indicate higher potency in inhibiting cancer cell proliferation. Compound **8m**, with an IC_{50} value of 23.00 ± 2.85, has a higher concentration requirement for 50% inhibition, suggesting lower potency compared to other 4-phenyl derivatives.

Overall, the 4-phenyl derivatives tend to exhibit slightly higher IC_{50} values compared to 4-methyl derivatives, suggesting that, on average, the 4-methyl series may have higher potency in inhibiting the growth of non-small cell lung cancer cells. The most potent compound overall is from the 4-methyl series (**8f** with 6.24 ± 1.91), while the least potent compound is from the 4-phenyl series (**8m** with 23.00 ± 2.85).

Colorectal cancer cell line (HCT-116): In the comparative analysis of 4-methyl and 4-phenyl derivatives, distinct trends in inhibitory activities against colorectal cancer cells are evident. Within the 4-methyl series, compounds such as **8j** (4-CF_3) and **8e** (4-OCH_3) exhibit exceptional potency, displaying the lowest IC_{50} values (4.85 ± 1.79 and 4.95 ± 1.82, respectively). The derivatives with substituents like 4-CN (**8f**), 4-CH_3 (**8b**) and 4-F (**8g**) manifest moderate to high inhibitory activities, with IC_{50} values ranging from 10.30 to 12.34. Conversely, compounds featuring 4-N$(CH_3)_2$ (**8d**), -H (**8a**), 4-OH (**8c**) and 4-Cl (**8h**) display moderate potency, with IC_{50} values ranging from 11.98 to 16.22. However, compound **8i** (4-NO_2) stands out with the highest IC_{50} value (23.91 ± 2.31), indicating comparatively lower potency within the 4-methyl series.

In 4-phenyl derivatives, compound **8e** (4-OCH_3) emerges as the most potent, showcasing the lowest IC_{50} value (17.54 ± 3.29). The inhibitory activities are observed in derivatives featuring 4-F (**8q**), 4-Cl (**8r**), 4-CH_3 (**8l**) and 4-N$(CH_3)_2$ (**8n**), with IC_{50} values ranging from 16.36 to 18.99. Conversely, compounds containing 4-NO_2 (**8s**), 4-CN (**8p**) and 4-CF_3 (**8t**) demonstrate moderate inhibitory activities, with IC_{50} values ranging from 16.72 to 18.15. Moreover, compounds **8k** (-H) and **8o** (4-OCH_3) within the 4-phenyl series exhibit higher IC_{50} values, indicating comparatively lower potency.

The 4-methyl derivatives showcase a broader spectrum of inhibitory activities, with compounds such as **8j** (4-CF_3) and **8e** (4-OCH_3) exhibiting high potency. In contrast, the 4-phenyl derivatives exhibit variability in inhibitory activities, with compound **8e** (4-OCH_3) standing out as highly potent. Both series comprise the compounds with noteworthy inhibitory activity against colorectal cancer cells.

Pancreatic cancer cell line (PANC-1): In the evaluation of IC_{50} values against the PANC-1 pancreatic cancer cell line, the 4-methyl derivatives revealed distinct inhibitory profiles. Notably, compounds **8f** (4-CN) and **8j** (4-CF_3) exhibited the highest potency, with an IC_{50} value of 6.75 ± 1.06, underscoring their robust inhibitory activity. Compound **8e** (4-OCH_3) demonstrated comparable efficacy, with a low IC_{50} value of 6.90 ± 1.09, indicative of significant inhibitory potential. Conversely, compound **8i** (4-NO_2) exhibited the least potency among the 4-methyl derivatives, with the highest IC_{50} value of 20.71 ± 3.47.

In case of 4-phenyl derivatives, compound **8n** (4-N-$(CH_3)_2$) and **8q** (4-F) showcased moderate inhibitory activity, while **8s** (4-NO_2) and **8o** (4-OCH_3) exhibited comparatively lower potency. These findings highlight the diverse inhibitory profiles within each derivative category. Compounds like **8e** (4-OCH_3) and **8j** (4-CF_3) emerge as promising candidates for further development as anti-pancreatic cancer agents.

Cervical cancer cell line (HaLa): The evaluation of IC_{50} values against the cervical cancer cell line (HaLa) reveals distinctive inhibitory profiles among the tested compounds. In the category of 4-methyl derivatives, compound **8h** (4-Cl) exhibits the highest potency with a remarkably low IC_{50} value of 8.07 ± 2.11, emphasizing its strong inhibitory activity against HaLa cells. Notably, compound **8e** (4-OCH_3) and **8j** (4-CF_3) also demonstrate noteworthy potency, with IC_{50} values of 11.98 ± 4.18 and 11.76 ± 4.09, respectively. Conversely, compound **8i** (4-NO_2) exhibits the highest IC_{50} value (30.76 ± 3.74) among the 4-methyl derivatives, indicating comparatively lower potency.

In case of 4-phenyl derivatives, compound **8k** (-H) and **8q** (4-F) showcase high potency with IC_{50} values of 28.12 ± 1.24 and 28.04 ± 2.69, respectively. However, the 4-phenyl derivatives also display variations in potency, as exemplified by compounds **8t** (4-CF_3) and **8m** (-4-OH) with IC_{50} values of 18.53 ± 1.13 and 19.80 ± 3.63, respectively. The impact of electron withdrawing and electron-donating groups on the anticancer activity of 4-methyl and 4-phenyl derivatives is evident from the IC_{50} values obtained for each compound against different cancer cell lines. In the context of the 4-methyl derivatives, it is observed that the introduction of electron donating groups, such as methyl (-CH_3) in compound **8b** (4-CH_3), methoxy (-OCH_3) in compound **8e** (4-OCH_3) and trifluoromethyl (CF_3) in compound **8j** (4-CF_3), contributes to higher potency against non-small cell lung cancer (A-549) and colorectal cancer (HCT-116) cells. These groups may enhance the electron density on the pyrimidine ring, promoting better interactions with the target cancer cells and thereby increasing the cytotoxic potential.

On the other hand, the electron-withdrawing group nitro (NO_2) in compound **8i** (4-NO_2) within the 4-methyl series exhibits lower potency, as indicated by the higher IC_{50} value against A-549 cells. This suggests that the electron-withdrawing nature of the nitro group may negatively impact the interactions with cancer cells, resulting in reduced cytotoxicity.

In the 4-phenyl derivatives, similar trends are observed. Compound **8e** (4-OCH_3) with an electron-donating methoxy group exhibits high potency against A-549 and HCT-116 cells. Conversely, compounds with electron-withdrawing groups, such as **8m** (4-OH) and **8s** (4-NO_2), display relatively lower potency against A-549 cells. The presence of electron-donating

or electron-withdrawing groups on the phenyl ring appears to influence the overall anticancer activity, potentially through modulation of molecular interactions with the target cancer cells. In comparison to 4-phenyl derivative series, the 4-methyl derivatives disclosed better anticancer potential indicating the importance of -CH_3 group at the 4th position of the pyrimidine ring system.

Conclusion

The synthesized novel pyrimidine tethered benzamide derivatives exhibited promising anticancer potential as evidenced by their strong binding affinities and cytotoxic effects against a range of cancer cell lines. Molecular docking studies revealed the importance of substituent groups in modulating interactions with target receptors, highlighting the need for further structure-activity relationship studies. Among the synthesized compounds, derivatives **8f** and **8j** emerged as the most promising anticancer agents against A-549 cells, compounds **8j** and **8e** showed exceptional potency against HCT-116 cells, compounds **8f** and **8j** demonstrated high efficacy against PANC-1 cells and compound **8h** displayed remarkable potency against HaLa cells. These compounds showed selectivity towards cancer cells while demonstrating lower cytotoxicity towards normal cells, indicating their potential as safe and effective anticancer agents. However, future research should focus on optimizing the pharmacokinetic properties of compounds (**8a-t**) and conducting *in vivo* studies to validate their therapeutic efficacy and safety profiles. Overall, this study lays the groundwork for the development of novel pyrimidine-tethered benzamide derivatives as targeted anticancer therapies.

ACKNOWLEDGEMENTS

The authors acknowledge the technical support provided by the Motherhood University in the completion of the research work.

CONFLICT OF INTEREST

The authors declare that there is no conflict of interests regarding the publication of this article.

REFERENCES

1. R.L. Siegel, K.D. Miller, N.S. Wagle and A. Jemal, *CA Cancer J. Clin.*, **73**, 17 (2023); https://doi.org/10.3322/caac.21763
2. A.M. Alafeefy, M. Ceruso, A.M. Al-Tamimi, S. Del Prete, C. Capasso and C.T. Supuran, *Bioorg. Med. Chem.*, **22**, 5133 (2014); https://doi.org/10.1016/j.bmc.2014.08.015
3. A.M. Alafeefy, M. Ceruso, N.A. Al-Jaber, S. Parkkila, A.B. Vermelho and C.T. Supuran, *J. Enzyme Inhib. Med. Chem.*, **30**, 581 (2015); https://doi.org/10.3109/14756366.2014.956309
4. J.K. DeMartino and D.L. Boger, *Drugs Future*, **33**, 969 (2008); https://doi.org/10.1358/dof.2008.033.11.1247542
5. W.J. Curran, *Oncology*, **63(Suppl. 2)**, 29 (2002); https://doi.org/10.1159/000067145
6. K. Nurgali, R.T. Jagoe and R. Abalo, *Front. Pharmacol.*, **9**, 245 (2018); https://doi.org/10.3389/fphar.2018.00245
7. S.M. El-Messery, G.S. Hassan, M.N. Nagi, E.E. Habib, S.T. Al-Rashood and H.I. El-Subbagh, *Bioorg. Med. Chem. Lett.*, **26**, 4815 (2016); https://doi.org/10.1016/j.bmcl.2016.08.022
8. C.L. Arteaga and D.H. Johnson, *Curr. Opin. Oncol.*, **13**, 491 (2001); https://doi.org/10.1097/00001622-200111000-00012
9. A.J. Barker, K.H. Gibson, W. Grundy, A.A. Godfrey, J.J. Barlow, M.P. Healy, J.R. Woodburn, S.E. Ashton, B.J. Curry, L. Scarlett, L. Henthorn and L. Richards, *Bioorg. Med. Chem. Lett.*, **11**, 1911 (2001); https://doi.org/10.1016/S0960-894X(01)00344-4
10. G. Joshi, H. Nayyar, S. Kalra, P. Sharma, A. Munshi, S. Singh and R. Kumar, *Chem. Biol. Drug Design*, **90**, 995 (2017); https://doi.org/10.1111/cbdd.13027
11. A.S. El-Azab, M.A. Al-Omar, A.A. Abdel-Aziz, N.I. Abdel-Aziz, M.A. El-Sayed, A.M. Aleisa, M.M. Sayed-Ahmed and S.G. Abdel-Hamide, *Eur. J. Med. Chem.*, **45**, 4188 (2010); https://doi.org/10.1016/j.ejmech.2010.06.013
12. S. Tiwari, S. Sachan, A. Mishra, S. Tiwari, V. Pandey and, *J. Int. Pharm. Life Sci.*, **6**, 4819 (2015).
13. I.A. Al-Suwaidan, A.A. Abdel-Aziz, T.Z. Shawer, R.R. Ayyad, A.M. Alanazi, A.M. El-Morsy, M.A. Mohamed, N.I. Abdel-Aziz, M.A.-A. El-Sayed and A.S. El-Azab, *J. Enzyme Inhib. Med. Chem.*, **31**, 78 (2016); https://doi.org/10.3109/14756366.2015.1004059
14. A. Ammazzalorso, M. Agamennone, B. De Filippis and M. Fantacuzzi, *Molecules*, **26**, 1488 (2021); https://doi.org/10.3390/molecules26051488
15. T.V. Sreevidya, B. Narayana and H.S. Yathirajan, *Cent. Eur. J. Chem.*, **8**, 174 (2010); https://doi.org/10.2478/s11532-009-0124-x
16. S. Narwal, S. Kumar and P.K. Verma, *Chem. Cent. J.*, **11**, 52 (2017); https://doi.org/10.1186/s13065-017-0284-2
17. J.A. Greenberg and T. Sammakia, *J. Org. Chem.*, **82**, 3245 (2017); https://doi.org/10.1021/acs.joc.6b02931
18. J.K. Park, W.K. Shin and D.K. An, *Bull. Korean Chem. Soc.*, **34**, 1592 (2013); https://doi.org/10.5012/bkcs.2013.34.5.1592
19. X.Y. Meng, H.X. Zhang, M. Mezei and M. Cui, *Curr. Computeraided Drug Des.*, **7**, 146 (2011); https://doi.org/10.2174/157340911795677602
20. T.L. Riss, R.A. Moravec, A.L. Niles, S. Duellman, H.A. Benink, T.J. Worzella, L. Minor, in eds.: S. Markossian, A. Grossman, M. Arkin, D. Auld, C. Austin, J. Baell, K. Brimacombe, T.D.Y. Chung, N.P. Coussens, J.L. Dahlin, V. Devanarayan, T.L. Foley, M. Glicksman, K. Gorshkov, J.V. Haas, M.D. Hall, S. Hoare, J. Inglese, P.W. Iversen, M. Lal-Nag, Z. Li, J.R. Manro, J. McGee, O. McManus, M. Pearson, T. Riss, Peter Saradjian, G.S. Sittampalam, M. Tarselli, O.J. Trask Jr., J.R. Weidner, M.J. Wildey, K. Wilson, M. Xia and X. Xu, Cell Viability Assays-Assay Guidance Manual, NCBI Bookshelf (2016).